Coherence-Based Operational Nonclassicality Criteria

Luca Innocenti,[1,2,*] Lukáš Lachman,[1] and Radim Filip[1]
[1]*Department of Optics, Palacký University, 17. Listopadu 12, 771 46 Olomouc, Czech Republic*
[2]*Università degli Studi di Palermo, Dipartimento di Fisica e Chimica–Emilio Segrè, via Archirafi 36, I-90123 Palermo, Italy*

(Received 12 October 2022; revised 15 March 2023; accepted 13 September 2023; published 18 October 2023)

The nonclassicality of quantum states is a fundamental resource for quantum technologies and quantum information tasks, in general. In particular, a pivotal aspect of quantum states lies in their coherence properties, encoded in the nondiagonal terms of their density matrix in the Fock-state bosonic basis. We present operational criteria to detect the nonclassicality of individual quantum coherences that use only data obtainable in experimentally realistic scenarios. We analyze and compare the robustness of the nonclassical coherence aspects when the states pass through lossy and noisy channels. The criteria can be immediately applied to experiments with light, atoms, solid-state system, and mechanical oscillators, thus providing a toolbox allowing practical experiments to more easily detect the nonclassicality of generated states.

DOI: 10.1103/PhysRevLett.131.160201

Introduction.—The nonclassicality of quantum states is of utmost importance for quantum information tasks [1], ranging from quantum communication and computation [2–5], quantum sensing [6], and thermodynamics [7]. For bosonic systems, a common definition of nonclassicality is the indivisibility of single bosons [8–11]. Another standard approach in quantum optics is to define a state ρ as nonclassical if it cannot be written as a convex decomposition of coherent states [12–14]:

$$\rho = \int d^2\alpha P(\alpha)|\alpha\rangle\langle\alpha| \tag{1}$$

for some non-negative probability distribution P [12,15,16]. This is referred to as P *nonclassicality* [17,18] and is the kind of nonclassicality that will be the focus of this Letter. Some further details about the formal definition of P nonclassicality are reviewed in Supplemental Material [19]. Note how the definition of P nonclassicality we study here differs from the one used in the context of resource theories of coherence [20]. For example, a classical state can have nondiagonal matrix components in the Fock-state basis, and pure Fock states are highly nonclassical. On the other hand, resource theories of coherence might consider states like $|1\rangle$ as "classical" [20]. Operationally, coherent states $|\alpha\rangle$ are ideal states of a linear oscillator driven by external coherent force. In general, reconstructing the P function experimentally is highly nontrivial [21,22]. Proposed criteria to detect P nonclassicality include witnesses relying on bounds on expectation values with respect to the P function [23,24] and hierarchies of necessary and sufficient nonclassicality criteria based on the moments of distribution [25–29], among other approaches [30–34]. These methods share the shortcoming of relying on *global* properties of the state, such as statistical moments, rather than being tailored to information directly accessible experimentally. Other nonclassicality criteria, based on photon-click statistics [35–40], are based on operationally measurable quantities but are tied to specific detection schemes.

As of yet, no nonclassicality criterion specifically tailored at individual quantum coherences—thus, not requiring an extensive characterization of the state—is known. A possible reason for this is that, while the shape of the set of classical states when only diagonal matrix elements are being observed is relatively manageable via generalized Klyshko-like inequalities [18,41], finding similar inequalities when coherences are also involved is highly nontrivial. However, quantum coherences being a useful resource for a variety of quantum information tasks [20,42], understanding the nonclassicality involving individual coherences would be valuable from both experimental and fundamental viewpoints. In this Letter, we lay out a framework to characterize the P nonclassicality using operationally accessible Fock-state quantum coherences. This allows us to discuss the role of coherence-based observables in certifying incompatibility with classical states of the form (1). Simultaneously, this enables us to establish experimental tasks in which the coherence among Fock states represents a necessary requirement for P-nonclassicality certification or enhances the capability to manifest such P nonclassicality. By contrast, criteria reliant only on Fock state probabilities [18] remain insensitive to this coherence. To ensure seamless applicability to experimental scenarios, our criteria exploit only knowledge of the expectation values of few observables, as one would have access to in realistic circumstances. To achieve this, we devise an approach to nonclassicality detection based on incomplete knowledge of the density matrix [18,43], extending the current state of the art by analyzing the information hidden in off-diagonal terms. These elements are directly measurable by Ramsey-like interferometry of trapped ion [44], superconducting circuit experiments [45], and electromechanical oscillators [46]. For light, atomic ensembles, and optomechanical oscillators, they can be reconstructed using homodyne tomography. We compare our criteria to those relying only on Fock-state probabilities [18,41] and analyze the nonclassical depth of various quantum coherences represented by different off-diagonal elements.

We find that observing coherence terms can provide enhanced predictive power in terms of nonclassicality detection compared to the information provided by only Fock-state probabilities [18] and showcase this in several instances of nonclassicality in one-, two-, and three-dimensional spaces. More precisely, we find that Fock-state probabilities alone are sometimes sufficient to detect nonclassicality, whereas in other situations knowledge about coherences provides enhanced predictive power. We show how each set of different measured observables provides a distinct boundary of nonclassicality and study the behavior in these spaces of superposition states subject to attenuation and thermal noise. This highlights how different types of noise affect the observable nonclassicality in nontrivial ways even in low-dimensional spaces.

General framework: Support function and support hyperplanes.—Suppose we are given the expectation values $\langle \mathcal{O}_i \rangle$ for some set of observables $\mathcal{O}_i$ and want to determine whether they are compatible with *some* classical state. Given the relevant Hilbert space $\mathcal{H}$, denote with $\mathcal{Q}$ the set of density matrices and with $\mathcal{C} \subset \mathcal{Q}$ the closure of the convex hull of the coherent states in $\mathcal{Q}$. Let us also denote with $\boldsymbol{O}(\rho) \equiv [\mathrm{Tr}(\mathcal{O}_k \rho)]_{k=1}^n$ the set of expectation values obtained measuring ρ. We seek a method to determine whether, given an unknown state ρ, there is $\sigma \in \mathcal{C}$ compatible with the observed measurements, that is, whether $\boldsymbol{O}(\rho) \in \{\boldsymbol{O}(\sigma) : \sigma \in \mathcal{C}\}$.

The convexity of $\mathcal{C}$ and $\mathcal{Q}$ allows one to characterize them via supporting hyperplanes, using the tools of convex geometry [47]. Any closed convex set $A \subset \mathbb{R}^n$ is characterized by its *support function* $h_A : \mathbb{R}^n \to \mathbb{R}$, defined as $h_A(\boldsymbol{n}) = \sup_{\boldsymbol{x} \in A} \langle \boldsymbol{n}, \boldsymbol{x} \rangle$. Geometrically, $h_A(\boldsymbol{n})$ represents the distance from the origin to the hyperplane tangent to A orthogonal to $\boldsymbol{n}$. To devise criteria with direct operational applicability, we consider the projection of $\mathcal{C}$, $\mathcal{Q}$ onto the finite-dimensional subspaces spanned by the measured observables. We then denote with $h_{\mathcal{C}}(\boldsymbol{n})$ and $h_{\mathcal{Q}}(\boldsymbol{n})$ the support functions of $\mathcal{C}$ and $\mathcal{Q}$ within these projected spaces. These support functions characterize everything about the boundary of $\mathcal{C}$, $\mathcal{Q}$ that can be inferred from the few measured observables. The task of nonclassicality detection, thus, translates into determining whether there is $\boldsymbol{n}$ such that $h_{\mathcal{Q}}(\boldsymbol{n}) > h_{\mathcal{C}}(\boldsymbol{n})$. Whenever this is the case, it is possible to find a set of measurement results $\boldsymbol{O} \in \mathbb{R}^n$ such that $\boldsymbol{n} \cdot \boldsymbol{O} > h_{\mathcal{C}}(\boldsymbol{n})$, which certifies that these measurement results are not compatible with any classical state. By studying the structure of $h_{\mathcal{C}}(\boldsymbol{n})$ and $h_{\mathcal{Q}}(\boldsymbol{n})$, we fully characterize the geometry of the $\mathcal{C}$ accessible from measurements. In some cases, this can lead to Klyshko-like nonclassicality criteria [18,41]. Notably, in many of the scenarios considered here, we will derive the criteria without explicitly involving the support function. This is possible in sufficiently simple situations where we can devise *ad hoc* procedures to reach a conclusion. Such *ad hoc* derivations can be regarded as a way to achieve a full characterization of $h_{\mathcal{C}}(\boldsymbol{n})$ for all of $\boldsymbol{n}$. Directly using the support function remains nonetheless very useful, as we will show in some explicit cases. While some of the underlying geometric insight was previously discussed in [18], considering coherences makes the task significantly more difficult and reveals interesting new phenomenology, on top of the clear advantages in applicability when measuring coherences is experimentally viable.

Computing $h_{\mathcal{Q}}(\boldsymbol{n})$ is generally easier, requiring finding the largest eigenvalue of $\boldsymbol{n} \cdot \boldsymbol{O} \equiv \sum_i n_i \mathcal{O}_i$, that is, computing the operator norm $\|\boldsymbol{n} \cdot \boldsymbol{O}\|_{\mathrm{op}}$. Nonetheless, this does not trivially translate into an algebraic characterization of the boundary of $\mathcal{Q}$, which requires solving such maximization for all $\boldsymbol{n}$. Computing $h_{\mathcal{C}}(\boldsymbol{n})$ is, in general, also difficult, requiring one to maximize $\sum_i n_i \mathrm{Tr}(\mathcal{O}_i \rho)$ over all $\rho \in \mathcal{C}$. We show here how to tackle these tasks in several cases of interest.

Coherence terms.—To focus on the nonclassicality of coherences, we consider as basic observables $X_{jk} \equiv |j\rangle\langle k| + |k\rangle\langle j|$ and $Y_{jk} \equiv i(|k\rangle\langle j| - |j\rangle\langle k|)$, which generalize nondiagonal Pauli matrices in higher dimensions. These capture coherence information not directly accessible via the Fock-state number probabilities $P_j \equiv |j\rangle\langle j|$. The expectation values of X_{jk} and Y_{jk} on a coherent state $|\alpha\rangle$, with $\alpha = \sqrt{\mu} e^{i\phi}$, are related to P_i as

$$
\begin{aligned}
X_{ij} &= 2\sqrt{P_i P_j} \cos[\phi(i-j)], \\
Y_{ij} &= 2\sqrt{P_i P_j} \sin[\phi(i-j)].
\end{aligned} \tag{2}
$$

For ease of notation, here and in the rest of the Letter, we will with some abuse of notation conflate the operators X_{jk} with their expectation values on a given state ρ, $\langle X_{jk} \rangle_\rho \equiv \mathrm{Tr}(X_{jk}\rho)$. For example, Eq. (2) would be more precisely written as $\langle X_{jk} \rangle_\alpha = 2\sqrt{\langle P_j \rangle_\mu \langle P_k \rangle_\mu} \cos[\phi(j-k)]$. More generally, we can consider the rotated operators $R_{jk}(\theta) \equiv \cos(\theta) X_{jk} + \sin(\theta) Y_{jk}$, whose expectation value on coherent states reads $R_{jk}(\theta) = 2\sqrt{P_j P_k} \cos[\theta - \phi(j-k)]$.

Quantum boundary.—When dealing with only Fock-state probabilities, any probability distribution is compatible with some quantum state, and, thus, the boundary of $\mathcal{Q}$ is simply defined by the relations $\sum_j P_j \leq 1$ and $0 \leq P_j \leq 1$. The situation changes significantly when coherence terms are considered. Finding the boundary of $\mathcal{Q}$ then amounts to figuring out the conditions under which the observed expectation values fit into a positive semidefinite matrix. We refer to Supplemental Material [19] for further details.

Nonclassicality criteria.—We will discuss here the nonclassicality certifiable via nondiagonal elements of the density matrix in the Fock-state basis, as well as the nonclassicality encoded in nontrivial combinations of different coherence terms, or in nontrivial combinations of both coherence terms and Fock-state probabilities.

One-dimensional criteria.—We first study nonclassicality criteria associated with individual coherence terms $R_{jk}(\theta)$. These are the easiest to apply in any experimental scenario where coherences are measured. In these spaces, the set of all states is bounded by $|R_{jk}(\theta)| \leq 1$, with bound saturated by the state $(1/\sqrt{2})(|j\rangle + e^{i\theta}|k\rangle)$. On the other hand, the corresponding classical bound is

$$|R_{jk}(\theta)| \leq \max_{\rho\in\mathcal{C}} 2\sqrt{\rho_{jj}\rho_{kk}} = 2e^{-(j+k)/2}\frac{[(j+k)/2]^{(j+k)/2}}{\sqrt{j!k!}}, \tag{3}$$

where the maximization can be restricted to the set of coherent states. The corresponding bound for the set of *all* states is instead $|R_{jk}(\theta)| \leq 1$, saturated by the state $(1/\sqrt{2})(|j\rangle + e^{i\theta}|k\rangle)$. In particular, we have

$$|X_{01}| \leq \sqrt{2}e^{-1/2} \approx 0.86, \qquad |X_{02}| \leq \sqrt{2}e^{-1} \approx 0.52,$$
$$|X_{12}| \leq \frac{\sqrt{27}}{2}e^{-3/2} \approx 0.58. \tag{4}$$

This means that, e.g., measuring any value for the coherence of $0.87 \leq |X_{01}| \leq 1$ is sufficient to certify nonclassicality. We refer to states violating any such inequality as displaying *nonclassical coherence*. As an interesting example showcasing the nontriviality of nonclassical coherences, consider any ρ that is a mixture of the nonclassical state $|1\rangle$ with any classical ρ_{cl}. Although such ρ might be recognizable as nonclassical via some observable, because only ρ_{cl} produces coherence terms, it will not display any *nonclassical coherences*, meaning it is not recognizable as nonclassical by any criterion involving only coherence terms. This example again highlights the contrast between resource-theoretic definitions of "nonclassical coherence," in which Fock states like $|1\rangle$ are "classical," and the quantum optical perspective, in which they are instead nonclassical by definition, and when mixed with a classical state ρ_{cl} can result in states whose nonclassicality can be probed only via coherence measurements.

Two-dimensional criteria.—Even though one-dimensional criteria using individual coherences can always be applied, we can devise stronger criteria characterizing higher-dimensional boundaries. This allows detecting as nonclassical states whose nonclassicality could not be deduced from any individual coherence term. For example, when measuring the pair of coherences (X_{jk}, Y_{jk}), $\mathcal{Q}$ is characterized by the inequality $X_{jk}^2 + Y_{jk}^2 \leq 1$, saturated by states of the form $(1/\sqrt{2})(|j\rangle + e^{i\theta}|k\rangle)$ for all $\theta \in [0, 2\pi]$. On the other hand, $\mathcal{C}$ only forms a circle of radius given by Eq. (3). It follows that measuring any pair of values for (X_{jk}, Y_{jk}) that falls outside such circle is sufficient to certify the nonclassicality of the underlying state.

One can also ask what nonclassicality is encoded in pairs of observables including both coherences and Fock probabilities. Consider, for example, some $R_{jk}(\theta)$ together with P_j. The boundary of $\mathcal{Q}$ corresponds to

$$|R_{jk}(\theta)| \leq \max_{P_k} 2\sqrt{P_j P_k} = 2\sqrt{P_j(1-P_j)}, \tag{5}$$

where the maximum is taken with respect to all nonnegative reals P_k such that $P_j + P_k \leq 1$ [that is, over all quantum states compatible with the given values of P_j and $R_{jk}(\theta)$]. On the other hand, classical states provide a generally more complex boundary. For example, in the space (P_0, X_{01}), the boundary is defined by the inequalities $0 \leq P_0 \leq 1$ and

$$0 \leq |X_{01}| \leq 2P_0\sqrt{-\log P_0}, \tag{6}$$

with the latter saturated by coherent states. Equation (6) means that there are states whose nonclassicality cannot be detected measuring P_0, nor measuring X_{01} and applying Eq. (4), but is nonetheless revealed properly exploiting the knowledge of both P_0 and X_{01}. An explicit example of this is measuring $P_0 = 0.2$ and $X_{01} = 0.6$, where we do not detect nonclassicality using only P_0 or X_{01}, but we do via criterion in the two-dimensional space (P_0, X_{01}).

In Fig. 1, we show how the nonclassicality criteria look like in two-dimensional spaces involving coherence terms and highlight the nonclassicality threshold corresponding to the one-dimensional criterion with X_{01}. This corresponds to projecting each of the given plots onto the horizontal axis. Further details on these criteria and their derivation is found in Supplemental Material [19]. Figure 1 shows that measuring coherence terms provides valuable nonclassicality information. This is reflected in the blue solid line in the figures being a strict subset of the gray solid line. This means that measuring any pair of expectation values to be outside of the blue region is sufficient to certify the nonclassicality of the underlying state, thus making for criteria directly usable in experiments.

Three-dimensional criteria.—Another interesting case is obtained considering both Fock-state probabilities and coherences. For example, in the space $(P_0, P_1, X_{01}, Y_{01})$, the set $\mathcal{Q}$ is characterized by the trivial constraint

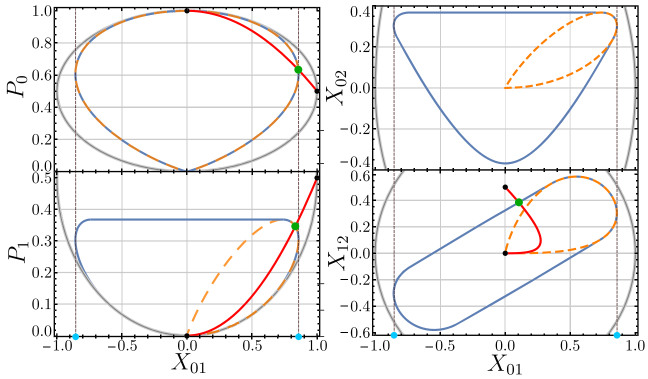

FIG. 1. Classical regions in the spaces (X_{01}, P_0), (X_{01}, P_1), (X_{01}, X_{02}), and (X_{01}, X_{12}). Solid blue lines trace the boundary of $\mathcal{C}$. Dashed orange lines are the set of *coherent* states of the form $|\sqrt{\mu}\rangle$ for $\mu \in \mathbb{R}$. Outer gray lines are the boundary of $\mathcal{Q}$. In (X_{01}, P_i), the solid red line corresponds to $(1/\sqrt{2})(|0\rangle + |1\rangle)$ attenuated through a beam splitter with transmissivity $T = |t|^2$, for $T \in [0, 1]$. The two black dots joined by this line correspond to the states $|+\rangle$ and $|0\rangle$. The green dot marks the transmissivity corresponding to a transition between classicality and nonclassicality and corresponds to $T \approx 0.73$ in (X_{01}, P_0) and $T \approx 0.69$ in (X_{01}, P_1), respectively. We also show the results of attenuating $(1/\sqrt{2})(|1\rangle + |2\rangle)$ in the (X_{01}, X_{12}) space. The nonclassicality threshold, again marked with a green dot, corresponds to $T \approx 0.84$. The cyan dots at the bottom of the lowermost figure correspond to the one-dimensional nonclassicality threshold for the coherence term X_{01}, corresponding to $X_{01} \approx \pm 0.86$.

$0 \leq P_0 + P_1 \leq 1$ on the probabilities, with the additional constraint

$$X_{01}^2 + Y_{01}^2 \leq 4P_0P_1 \Leftrightarrow |R_{01}(\theta)| \leq 2\sqrt{P_0P_1} \quad \forall\ \theta. \qquad (7)$$

Thus, in this space, $\mathcal{Q}$ is a disk with radius $2\sqrt{P_0P_1}$. More rigorously, as discussed in Supplemental Material [19], this constraint follows from Sylvester's criterion for positive semidefiniteness [48]. We thus find that, remarkably, albeit it is possible to detect a state as nonclassical using the values of P_0 and P_1, if using these values it is *not* possible to detect the state as nonclassical, then it will still not be possible to do so adding knowledge about X_{01} and Y_{01}. With such analysis, we are thus able to predict which observables will be useful for the purpose of identifying nonclassicality, which helps to devise more efficient experimental platforms.

In other cases, for example, when one knows (P_0, P_2) but not P_1, the associated coherence terms do provide information about nonclassicality. This can be traced down to the boundary of $\mathcal{C}$ in the space (P_0, P_2) containing nonpure states and to the nonconvexity of the set of coherent states in the same space. Remarkably, in this case, adding knowledge of R_{02} allows one to recognize as nonclassical states in the nonconvex region of the space (P_0, P_2). Further discussion of this aspect is provided in Supplemental Material [19].

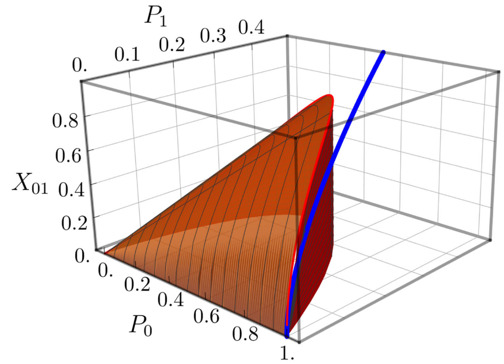

FIG. 2. Boundary of $\mathcal{C}$ in the subspace (P_0, P_1, X_{01}). The dashed red line represents the attenuated states obtained from $(1/\sqrt{2})(|0\rangle + |1\rangle)$, for different degrees of attenuations. The orange surfaces correspond to $\mathcal{C}$ in this subspace. The vertical orange surface corresponds to the criterion in the (P_0, P_1) subspace, while the other surface is the one bounding the value of $|X_{01}|$ for each value of (P_0, P_1). Nonclassicality is, thus, certified by checking that a point lies beyond at least one of these two surfaces.

These case studies highlight the nontrivial features of nonclassical coherences that set them apart from previously known nonclassicality criteria [18,41].

Robustness of nonclassical coherences.—To probe the robustness of the criteria, we also study how different degrees of attenuation and thermal noise affect our capacity to detect the nonclassicality of coherent states. Figure 1 shows attenuated superpositions in two-dimensional subspaces. In Figs. 1(a) and 1(b), we plot the points corresponding to attenuation of $(1/\sqrt{2})(|0\rangle + |1\rangle)$ with transmittivities $T \in [0, 1]$. We find that nonclassicality can be certified using (P_0, X_{01}) for $T > 0.73$, while in (P_1, X_{01}) for $T > 0.69$. In Fig. 1(d), we plot attenuated states obtained from $(1/\sqrt{2})(|1\rangle + |2\rangle)$. In this case, we

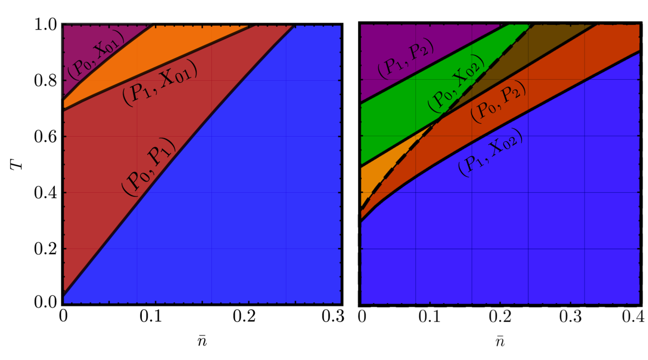

FIG. 3. Nonclassicality of $(1/\sqrt{2})(|0\rangle + |1\rangle)$ (left) and $(1/\sqrt{2})(|0\rangle + |2\rangle)$ (right) after attenuation with transmissivity $T \equiv |t|^2$ and thermalization with average boson number $\bar{n}$. Each line corresponds to a different two-dimensional nonclassicality criterion, separating the lower-right region of nonclassicality from the rest.

find the nonclassicality threshold in the space (X_{01}, X_{12}) to sit at around $T \approx 0.84$. We furthermore analyze the robustness of states obtained from $(1/\sqrt{2})(|0\rangle + |1\rangle)$ and $(1/\sqrt{2})(|0\rangle + |2\rangle)$ when subject to both attenuation and thermal noise. As shown in Figs. 2 and 3, different combinations of observables result in different nontrivial nonclassicality criteria, highlighting how the hardness in witnessing nonclassicality depends on the measured observables.

Conclusions.—We showed how to leverage individual off-diagonal elements of the density matrix in the Fock-state basis to assess P nonclassicality and how to pair these with Fock-state probabilities to detect even larger classes of nonclassical states. This paves the way for a more thorough understanding of the relation between P nonclassicality and the widely studied resource theories of quantum coherence [20].

These criteria can be directly implemented experimentally, by simply measuring the relevant observables and checking whether the obtained expectation values violate the given criteria. Such a protocol can be implemented with state-of-the-art technology, for example, in photonics [49], trapped ions [44], superconducting [45], and electromechanical [46] platforms. Enhanced capabilities of detecting nonclassical states have several applications, for example, for quantum metrology [44,50,51] and for quantum communication and computation [52,53]. Our results highlight the nontrivial way the nonclassicality of states is encoded in the coherences: While measuring coherences provides useful information in many situations, there also exist scenarios where all the information about nonclassicality is already encoded in the Fock-state probabilities. This leaves open the stimulating question of characterizing the scenarios where coherent terms do or do not provide additional predictive power.

Our Letter also paves the way for a more thorough understanding of nonclassicality detection with multimode coherences over diverse platforms [54–59]. Such criteria would provide enhanced detection schemes for platforms generating entangled states, imposing more lenient demands on those sources than entanglement. Another natural venue of further study is to devise criteria for quantum non-Gaussianity [40,60] and study the role of coherences in that context, which remains not fully understood.

L. I. acknowledges support from MUR and AWS under Project PON Ricerca e Innovazione 2014-2020, “calcolo quantistico in dispositivi quantistici rumorosi nel regime di scala intermedia” (NISQ—Noisy, Intermediate-Scale Quantum) and support from MEYS CR and the European Union’s Horizon 2020 (2014–2020) research and innovation framework programme under Grant Agreement No. 731473 (Project No. 8C20002 ShoQC). Project ShoQC has received funding from the QuantERA ERA-NET Cofund in Quantum Technologies implemented within the European Union’s Horizon 2020 Programme. L. L. and R. F. acknowledge Project No. 21-13265X of the Czech Science Foundation. We additionally acknowledge the EU H2020-WIDESPREAD-2020-5 project NONGAUSS (951737) under the CSA-Coordination and Support Action.

*luca.innocenti@unipa.it

[1] B. Yadin, F. C. Binder, J. Thompson, V. Narasimhachar, M. Gu, and M. S. Kim, Phys. Rev. X **8**, 041038 (2018).
[2] E. Knill, R. Laflamme, and G. J. Milburn, Nature (London) **409**, 46 (2001).
[3] P. Kok, W. J. Munro, K. Nemoto, T. C. Ralph, J. P. Dowling, and G. J. Milburn, Rev. Mod. Phys. **79**, 135 (2007).
[4] N. Gisin and R. Thew, Nat. Photonics **1**, 165 (2007).
[5] J. Shapiro, IEEE J. Sel. Top. Quantum Electron. **15**, 1547 (2009).
[6] C. L. Degen, F. Reinhard, and P. Cappellaro, Rev. Mod. Phys. **89**, 035002 (2017).
[7] G. Maslennikov, S. Ding, R. Hablützel, J. Gan, A. Roulet, S. Nimmrichter, J. Dai, V. Scarani, and D. Matsukevich, Nat. Commun. **10**, 1 (2019).
[8] R. Hanbury Brown and R. Q. Twiss, Nature (London) **178**, 1046 (1956).
[9] H. J. Kimble, M. Dagenais, and L. Mandel, Phys. Rev. Lett. **39**, 691 (1977).
[10] R. Short and L. Mandel, Phys. Rev. Lett. **51**, 384 (1983).
[11] S. Hong, R. Riedinger, I. Marinković, A. Wallucks, S. G. Hofer, R. A. Norte, M. Aspelmeyer, and S. Gröblacher, Science **358**, 203 (2017).
[12] R. J. Glauber, Phys. Rev. **131**, 2766 (1963).
[13] L. Mandel and E. Wolf, *Optical Coherence and Quantum Optics* (Cambridge University Press, Cambridge, England, 1995).
[14] W. Vogel and D.-G. Welsch, *Quantum Optics* (John Wiley & Sons, New York, 2006).
[15] E. C. G. Sudarshan, Phys. Rev. Lett. **10**, 277 (1963).
[16] K. C. Tan and H. Jeong, AVS Quantum Sci. **1**, 014701 (2019).
[17] F. Albarelli, A. Ferraro, M. Paternostro, and M. G. A. Paris, Phys. Rev. A **93**, 032112 (2016).
[18] L. Innocenti, L. Lachman, and R. Filip, npj Quantum Inf. **8**, 1 (2022).
[19] See Supplemental Material at http://link.aps.org/supplemental/10.1103/PhysRevLett.131.160201 for more details.
[20] A. Streltsov, G. Adesso, and M. B. Plenio, Rev. Mod. Phys. **89**, 041003 (2017).
[21] T. Kiesel, W. Vogel, V. Parigi, A. Zavatta, and M. Bellini, Phys. Rev. A **78**, 021804(R) (2008).
[22] T. Kiesel, W. Vogel, M. Bellini, and A. Zavatta, Phys. Rev. A **83**, 032116 (2011).
[23] T. Richter and W. Vogel, Phys. Rev. Lett. **89**, 283601 (2002).
[24] J. K. Korbicz, J. I. Cirac, J. Wehr, and M. Lewenstein, Phys. Rev. Lett. **94**, 153601 (2005).
[25] G. S. Agarwal and K. Tara, Phys. Rev. A **46**, 485 (1992).
[26] E. V. Shchukin and W. Vogel, Phys. Rev. A **72**, 043808 (2005).

[27] E. Shchukin, T. Richter, and W. Vogel, Phys. Rev. A **71**, 011802(R) (2005).
[28] W. Vogel, Phys. Rev. Lett. **100**, 013605 (2008).
[29] A. Miranowicz, M. Bartkowiak, X. Wang, Y. X. Liu, and F. Nori, Phys. Rev. A **82**, 013824 (2010).
[30] Á. Rivas and A. Luis, Phys. Rev. A **79**, 042105 (2009).
[31] M. Bohmann and E. Agudelo, Phys. Rev. Lett. **124**, 133601 (2020).
[32] K. C. Tan, S. Choi, and H. Jeong, Phys. Rev. Lett. **124**, 110404 (2020).
[33] P. Grünwald, New J. Phys. **21**, 093003 (2019).
[34] P. Grünwald, Phys. Rev. Res. **2**, 023147 (2020).
[35] J. Sperling, W. Vogel, and G. S. Agarwal, Phys. Rev. Lett. **109**, 093601 (2012).
[36] J. Sperling, W. R. Clements, A. Eckstein, M. Moore, J. J. Renema, W. S. Kolthammer, S. W. Nam, A. Lita, T. Gerrits, W. Vogel *et al.*, Phys. Rev. Lett. **118**, 163602 (2017).
[37] R. Filip and L. Lachman, Phys. Rev. A **88**, 043827 (2013).
[38] L. Rigovacca, C. Di Franco, B. J. Metcalf, I. A. Walmsley, and M. S. Kim, Phys. Rev. Lett. **117**, 213602 (2016).
[39] L. Lachman and R. Filip, New J. Phys. **21**, 083012 (2019).
[40] L. Lachman, I. Straka, J. Hloušek, M. Ježek, and R. Filip, Phys. Rev. Lett. **123**, 043601 (2019).
[41] D. N. Klyshko, Phys. Lett. A **213**, 7 (1996).
[42] C. Lüders, M. Pukrop, F. Barkhausen, E. Rozas, C. Schneider, S. Höfling, J. Sperling, S. Schumacher, and M. Aßmann, arXiv:2209.07129.
[43] R. Filip and L. Mišta Jr, Phys. Rev. Lett. **106**, 200401 (2011).
[44] K. C. McCormick, J. Keller, S. C. Burd, D. J. Wineland, A. C. Wilson, and D. Leibfried, Nature (London) **572**, 86 (2019).
[45] L. Hu, Y. Ma, W. Cai, X. Mu, Y. Xu, W. Wang, Y. Wu, H. Wang, Y. Song, C.-L. Zou *et al.*, Nat. Phys. **15**, 503 (2019).
[46] Y. Chu, P. Kharel, T. Yoon, L. Frunzio, P. T. Rakich, and R. J. Schoelkopf, Nature (London) **563**, 666 (2018).
[47] D. Hug and W. Weil, *A Course on Convex Geometry* (Springer International, New York, 2020).
[48] C. R. Johnson and R. A. Horn, *Matrix Analysis* (Cambridge University Press, Cambridge, England, 1985).
[49] M. Yukawa, K. Miyata, T. Mizuta, H. Yonezawa, P. Marek, R. Filip, and A. Furusawa, Opt. Express **21**, 5529 (2013).
[50] H. Kwon, K. C. Tan, T. Volkoff, and H. Jeong, Phys. Rev. Lett. **122**, 040503 (2019).
[51] W. Wang, Y. Wu, Y. Ma, W. Cai, L. Hu, X. Mu, Y. Xu, Z.-J. Chen, H. Wang, Y. P. Song *et al.*, Nat. Commun. **10**, 4382 (2019).
[52] L. Li, C.-L. Zou, V. V. Albert, S. Muralidharan, S. M. Girvin, and L. Jiang, Phys. Rev. Lett. **119**, 030502 (2017).
[53] M. H. Michael, M. Silveri, R. T. Brierley, V. V. Albert, J. Salmilehto, L. Jiang, and S. M. Girvin, Phys. Rev. X **6**, 031006 (2016).
[54] S. A. Babichev, J. Appel, and A. I. Lvovsky, Phys. Rev. Lett. **92**, 193601 (2004).
[55] G. Thekkadath, M. Mycroft, B. Bell, C. Wade, A. Eckstein, D. Phillips, R. Patel, A. Buraczewski, A. Lita, T. Gerrits *et al.*, npj Quantum Inf. **6**, 1 (2020).
[56] Y. Y. Gao, B. J. Lester, Y. Zhang, C. Wang, S. Rosenblum, L. Frunzio, L. Jiang, S. M. Girvin, and R. J. Schoelkopf, Phys. Rev. X **8**, 021073 (2018).
[57] J. Zhang, M. Um, D. Lv, J.-N. Zhang, L.-M. Duan, and K. Kim, Phys. Rev. Lett. **121**, 160502 (2018).
[58] Y. Y. Gao, B. J. Lester, K. S. Chou, L. Frunzio, M. H. Devoret, L. Jiang, S. M. Girvin, and R. J. Schoelkopf, Nature (London) **566**, 509 (2019).
[59] H. Gan, G. Maslennikov, K.-W. Tseng, C. Nguyen, and D. Matsukevich, Phys. Rev. Lett. **124**, 170502 (2020).
[60] I. Straka, L. Lachman, J. Hloušek, M. Miková, M. Mičuda, M. Ježek, and R. Filip, npj Quantum Inf. **4**, 1 (2018).